STUDIA UNIVERSITATIS BABEŞ-BOLYAI, CHEMIA, XLV, 1-2, 2000

THE HYDROGEN PEROXIDE – IODIDE REACTION IN KINETIC ANALYSIS. AN ATTEMPT FOR MULTICOMPONENT CALIBRATION

ALEXANDRA RUSTOIU-CSAVDARI, IOAN BÂLDEA, LUCIAN COPOLOVICI, DANA MIHAI

"Babeş-Bolyai" University, Faculty of Chemistry and Chemical Engineering, Department of Physical Chemsitry, 11 Arany Janos Street, 3400 Cluj-Napoca
E-mail: arustoiu@chem.ubbcluj.ro

ABSTRACT. The applications of the Landolt-type hydrogen peroxide – iodide reaction has been extended to other species than those mentioned in the literature, such as vanadium, copper and iron. Detection of the incubation time was carried out visually. Reaction conditions towards Mo(VI) and V(V) were optimized and calibration lines t_0/t versus catalyst concentration were drawn. Further, the most often cited interferents, that is Cu(II) and Fe(III), were added to the reaction mixture and the joint behavior of V(V)-Cu(II), Cu(II)-Fe(III) and Mo(VI)-Cu(II)-Fe(III) matrixes have been studied. Their joint catalytic effect was proved to be neither additive nor synergistic. Bi-component and tri-component calibration models based on a t_0/t = f {[ion1],[ion2]} response surface or on a family of such surfaces respectively, were proposed. Results of visual and potentiometric detection of the reaction end-point were compared. The two methods have comparable performances.

Introduction

In recent years, kinetic or catalytic methods have opened a completely new area of research in analytical chemistry [1]. Within these, the analytical applications of Landolt reactions among chronometrical methods are obvious. Since the reaction time t decreases in the presence of a catalyst, it can be related to the catalyst concentration by means of $1/t$ or t_0/t versus analyte concentration calibration graphs. t_0 and t correspond to the absence and presence of the catalyst, respectively.

The slow oxidation of iodide by hydrogen peroxide in acidic medium to form iodine

$$2\ I^- + H_2O_2 + 2\ H^+ \rightarrow 2\ H_2O + I_2 \qquad (1)$$

was studied by many scientists [2], but the first to elucidate its mechanism and to give some kinetic parameters were Liebhafsky and Mohammed [3]. The following law can describe the reaction rate:

$$r = \frac{d[H_2O_2]}{dt} = k_2[H_2O_2][I^-] + k_4[H_2O_2][I^-][H^+] \qquad (2)$$

To serve the purpose of kinetic analysis, the hydrogen peroxide-iodide reaction can be easily transformed into a Landolt-type system by adding some trap for iodine (ascorbic acid [4,5] or thiosulfate [38]) to the reaction mixture. In the case of ascorbic acid for example, the iodine produced by reaction (1) will instantaneously be reduced back to iodide and dehydroascorbic acid will be released:

$$C_6H_8O_6 + I_2 \rightarrow 2\,H^+ + 2\,I^- + C_6H_6O_6 \qquad (3)$$

Therefore, as long as the ascorbic acid is not completely consumed, iodine does not accumulate. When it is totally consumed, I_2 is suddenly accumulated and the Landolt-effect [4,5] occurs. This phenomenon can easily be observed, even visually, because the mixture turns suddenly from colorless to yellow (which is typical for iodine), blue (in the presence of starch) or violet (in the presence of variamine blue). Yet, one may use any other indicator of the occurrence of the Landolt-effect. Its time lapse, also called "reaction time" ***t*** or "incubation time", depends on the concentration of the single reactants as well as on the concentration of any catalyst present in the mixture. Svehla [4], proved a linear dependence of ***t*** on the $C_6H_8O_6$ concentration as well as an exponential correlation with the I^- concentration. He also explained the linear dependence of ***1/t*** and t_0/t on the catalyst concentration, on the base of reaction kinetics and mechanism.

Reaction (1) is catalyzed by many metal ions in their higher oxidation states and was proposed as possible indicator reaction in kinetic analysis for the determination of Zr, Hf, Th, Ta, Mo, W and Fe by Yatsimirskii [6]. Mottola [8] added Pb and Ag to the list. Methods to determine some non-metallic catalysts, such as $Cr_2O_7^{2-}$ and PO_4^{3-} [9], were also reported.

Yet, in spite of the long list of metal ions above, the majority of catalytic methods based on the hydrogen peroxide – iodide Landolt-type reaction were developed to determine molybdenum [10-27], tungsten [26-29] or their mixtures [33-37]. However, analysis of iron [30], hafnium and zirconium [31] or joint determination of molybdenum–iron [32,38,39], molybdenum–copper [38,39] mixtures were also mentioned. The end-point of the reaction was detected visually [10,17-18,28,38-39], spectrophotometrically [15,34-37], potentiometrically [11-14,20,32-33], thermometrically [22] or amperometrically [19]. A large variety of samples were analyzed, such as water, food, vegetal material, minerals and steel.

Many of the methods are highly sensitive; detection limits as low as 0.7 μg/l [15] were reported. The most significant interferents for the determination of molybdenum are copper and iron, hence EDTA [14,20,29,32,38-39] is commonly used to remove their effect. Analysis of Mo(VI) is sometimes interfered by vanadium and tungsten [18] as well. Improvement of selectivity was also achieved either by removing the interferents during the pretreatment of samples [18,22-23] or by incorporating a cation-exchange resin column into the system [21]. Other scientists [27] preferred a mathematical correction of their calibration model.

During the 1970's, researchers were enthusiastic because of the simplicity of the principle and experimental device. By just using some temperature controlled vessels and a stopwatch (the so-called "clock method"), they were able to visualize the end-point of the reaction and develop some fairly sensitive kinetic methods [10]. However, during the years to come more performant and accurate apparatus replaced this tedious "monitoring" procedure. Nowadays, efforts concentrate rather on miniaturization [12-13,15] and automatization [9,13,15,21,25-26] of processes: samples can be as tiny as 100 μl [12] and sampling rates can reach up to 120 every hour [25].

Bi-component analysis, although it does not require pre-separation, it still needs two distinct experiments to determine the concentration of both analytes. One corresponds to the cumulative effect of both ions, while the other only to the effect of one of them. The catalytic effect of the second ion is removed by masking it. Thus, Mo(VI)-Fe(III) and Mo(VI)-W(VI) mixtures were analyzed by masking Fe(III) with EDTA [32] and Mo(VI) with citric acid [35], respectively. These procedures, however, rely on the additive joint effect of the catalysts. Recent methods not only deal with synergistic effects [36,37] by compensating the deviation from additivity within the calibration model *via* a synergistic catalytic coefficient, but also give the composition of the matrix by means of just one experiment.

The first purpose of this paper is to undertake the simple experimental device of the 1970's and extend the application of the hydrogen peroxide – iodide Landolt-type reaction to other bi- and tri-component mixtures, such as Cu(II)-Fe(III) and Mo(VI)-Cu(II)-Fe(III) as well as to other species, such as V(V) and its mixtures with Cu(II). The Mo(VI)-Cu(II) and Mo(VI)-Fe(III) couples exhibit an additive catalytic effect [38] for narrow concentration ranges. Hence, the second purpose was to enlarge the Cu(II) and Fe(III) concentration ranges to values where the joint effect of the catalyst is neither additive nor synergistic. Some attempts were also made to elaborate a suitable calibration model for Mo(VI)-Cu(II)-Fe(III) and V(V)-Cu(II) mixtures by obtaining the appropriate calibration surfaces or family of surfaces. Copper and iron were chosen as components of the mixtures because they are the most interferents in determination of molybdenum. Results of these simple kinetic experiments are verified by potentiometric runs for the case of Mo(VI) and some of its mixtures with Cu(II) and Fe(III).

Experimental

Reagents and Solutions

Analytical grade reagents provided by *Reactivul* (Bucharest, Romania), *Reanal* (Budapest, Hungary) and *Merck* (Darmstadt, Germany) were used without further purification. All solutions were prepared in twice distilled water produced by a VDB-3A glass device.

A stock solution of sulfuric acid was used as source of hydrogen ions. Ammonium molybdate $(NH_4)_6Mo_7O_{24}$, ammonium meta-vanadate NH_4VO_3, copper sulfate $CuSO_4.5H_2O$ and iron chloride $FeCl_3$ were used as sources for Mo(VI), V(V), Cu(II) and Fe(III) ions, respectively. Aqueous stock solutions of 10^{-2} mol.dm^{-3}

of all salts were prepared by dissolving the appropriate amount in volumetric flasks of various volumes, according to the needs of the experiments. Working solutions were obtained by adequate dilution of stock solutions. The Cu(II) concentration was determined by titration of the acid gained when 2 ml stock solution passed through a column of C-100H cationite resin (*Virolyte*, Victoria, Romania). The Fe(III) content of the acidulated iron chloride solution was determined by titration of the iodine obtained when 2 ml stock solution were mixed with KI and H_2SO_4. The acidity of this solution was also established. The solutions of hydrogen peroxide ascorbic acid or sodium ascorbate were freshly prepared before each set of experiments. The H_2SO_4 and H_2O_2 solutions were standardized by usual procedures. An aqueous 1 % wg. starch solution was used as color indicator for iodine.

Experimental device. Procedure

Experiments were carried out at constant temperature of 293 ± 0.1 K. Two solutions were prepared for each experiment, so that after mixing the total volume was of 20 ml. The oxidant solution ***A***, of 15 ml volume, contained H_2O_2, $Na_2C_6H_6O_6$ or $C_6H_8O_6$, H_2SO_4, starch and the catalyst, while the 5 ml of the reductant solution ***B*** contained only KI. Both were kept at controlled temperature as follows: solution ***A*** in a double wall glass vessel (which also served as reaction vessel) connected to a WOBSER U15 precision circulation bath, while solution ***B*** in a separate vessel kept in the water bath. The reaction vessel was placed on a magnetic stirrer. Solution ***B*** was injected into solution ***A*** under stirring and a precision stopwatch was started. Mixing time did not exceed 0.5-1 s. The reaction time ***t*** for the mixture to turn from colorless to blue, was recorded. Three to five replicate runs were carried out for each set of experimental conditions. Time measurements did not differ to more than ± 1 %.

Potentiometric runs were carried out with an electrochemical cell consisting of two temperature controlled glass vessels. One contained the reaction mixture and a working I^- - selective electrode, while the other a saturated calomel reference electrode. The electrodes were connected to a Radelkis multimeter. A bridge salt of saturated potassium nitrate was used to connect the half-cells. The electromotive force was monitored versus time. The *"Raluca Ripan" Chemical Research Institute* of Cluj-Napoca provided the electrodes. The solutions used in potentiometric experiments were prepared in demineralized and four time distilled water.

Results and discussions

The catalytic effect of molybdate on the hydrogen peroxide – iodide reaction is probably due to the rapid formation of peroxymolybdic acid [4,14], that further reacts slowly with iodide to regenerate the catalyst:

$$H_2O_2 + H_2MoO_4 \rightarrow H_2O_2 \bullet H_2MoO_4 \quad (4)$$

$$I^- + H_2O_2 \bullet H_2MoO_4 \rightarrow IO^- + H_2O + H_2MoO_4 \quad (5)$$

Iodine is formed from IO^-, so that the empirical reaction is the same as expressed in (1). Among the processes above, (5) is slow but much faster than its uncatalysed correspondent. The other steps occur rapidly. Thus, H_2MoO_4 is regenerated during

the entire cycle. Besides, combination of reactions (1) and (3) ensures constant I^- concentration in the reaction mixture.

Hence, in the presence of molybdate and under an excess acid concentration (or in buffer solution), the consumption rate of hydrogen peroxide [40] can be described as:

$$r = -\frac{d[H_2O_2]}{dt} = \left(k_{un} + k_{cat}[Mo(VI)]\right)[H_2O_2] \qquad (6)$$

where k_{un} stands for a pseudo-first order rate coefficient in the absence of the catalyst. On the other hand, k_{cat} stands for a second order rate coefficient of the molybdenum catalyzed reaction path.

Rate equation (6) can be integrated by considering that when reagents are mixed (time ***t*** = 0) $[H_2O_2] = [H_2O_2]_0$ and at the end of the induction period (time ***t***) $[H_2O_2] = [H_2O_2]_0 - [C_6H_8O_6]_0$ (the subscript indicates initial concentrations). This leads to

$$\frac{1}{t} = \frac{k_{un} + k_{cat}[Mo(VI)]}{\ln\left(\dfrac{[H_2O_2]_0}{[H_2O_2]_0 - [C_6H_8O_6]_0}\right)} \qquad (7)$$

Hence, the ratio $\boldsymbol{t_0/t}$ of reaction times recorded in the absence and presence of catalyst, can be expressed as

$$\frac{t_0}{t} = 1 + \frac{k_{cat}}{k_{un}}[Mo(VI)] \qquad (8)$$

It is obvious that linear calibration graphs may be obtained by plotting either ***1/t*** or $\boldsymbol{t_0/t}$ against the catalyst concentration. Svehla [10] proved that the $\boldsymbol{t_0/t}$ *vs* concentration plot is more independent of the individual time values, provided experimental conditions do not vary too much. Based on this as well as on its simplicity, we have chosen equation (18) as the base of calibration graphs for our analytical purposes.

Monocomponent calibration for Mo(VI), Cu(II), Fe(III) and V(V)

Molybdenum

Optimal reaction conditions regarding concentration of reagents were searched for in order to ensure a high sensitivity towards molybdenum, that is a high slope in equation (8). Therefore, kinetic runs were performed at various ascorbic acid, potassium iodide and sulfuric acid concentrations, for both in the absence and presence of 10^{-6} mole.dm^{-3} Mo(VI).

The mineral acid has to be in excess and the concentration of ascorbic acid should be two orders of magnitude smaller than that of hydrogen peroxide. The latter condition ensures less than 10 % reaction extent at the end-point. A small extent of the reaction presents the advantage that the side reactions, such as the decomposition of H_2O_2, will not affect the experimental results.

Because of practical reasons, an initial H_2O_2 concentration of 1.2×10^{-2} mole.dm^{-3} and a temperature of 293±0.1K were chosen for all experiments.

Experimental k_{cat}/k_{un} values (mean of at least three replicate runs) are presented in Table 1 along with the corresponding pH and ionic strength of the reaction mixture.

No precautions were taken to maintain the ionic strength. Its value is practically given by the contributions of KI and the acid. However, these species have always the same initial concentration for each set of measurements and in all cases the ionic strength is high enough to cover any possible contribution due to a water sample to be analyzed [41].

Table 1

Influence of reagent concentrations on the k_{cat}/k_{un} ratio at $1.2x10^{-2}$ mole.dm^{-3} H_2O_2 and 10^{-6} mole.dm^{-3} Mo(VI) at 293 ± 0.1 K.

Reaction conditions (concentrations given in mole.dm^{-3})	**Concentration of studied species (mole.dm^{-3})**	**10^{-5} x k_{cat}/k_{un} (dm^3.mole^{-1})**	**pH**	**Ionic strength (mole.dm^{-3})**
Effect of $Na_2C_6H_6O_6$: $[H_2SO_4]$ = 0.1 *[KI] = 3x10^{-3}* **[KI] = 6x10^{-3}**	*4x10^{-4}*	*5.80*	1.02	*0.19*
	8x10^{-4}	*2.80*		
	2x10^{-4}	**6.50**		**0.20**
	4x10^{-4}	**6.20 ***		
	6x10^{-4}	**4.10**		
Effect of KI : $[H_2SO_4]$ = 0.1 $[Na_2C_6H_6O_6]$ = 4x10^{-4}	3x10^{-3}	6.00	1.02	0.19
	6x10^{-3}	6.20 *		
	12x10^{-3}	6.50		0.20
Effect of H_2SO_4 : *$[Na_2C_6H_6O_6]$ = 4x10^{-4} [KI] = 6x10^{-3}* **$[Na_2C_6H_6O_6]$ = 8x10^{-4} [KI] = 1.2x10^{-3}**	*0.06*	*7.60*	*2.01*	*0.12*
	0.10	*6.20 **	*1.02*	*0.20*
	0.12	**0.80**	**0.96**	**0.24**
	0.16	**1.70**	**0.85**	**0.32**

** Labeled values in the third column correspond to identical reaction conditions.*

Table 2

Results of kinetic runs. Calibration for Mo(VI).
$1.2x10^{-2}$ mole.dm^{-3} H_2O_2, $6x10^{-3}$ mole.dm^{-3} KI, $6x10^{-2}$ mole.dm^{-3} H_2SO_4, $4x10^{-4}$ mole.dm^{-3} $Na_2C_6H_6O_6$ and ionic strength of 0.12 mole.dm^{-3} at 293 ± 0.17 K.

10^7 x [Mo(VI)] (mole.dm^{-3})	t (s)	Average t_0/t
0.0 (the blank run)	10 recordings average t_0 = 372 s	1.000
2.0	327, 328, 329	1.135
4.0	288, 290, 291	1.287
6.0	260, 261, 260	1.429
8.0	239, 237, 238	1.562
10.0	223, 220, 222	1.679

It may be observed from Table 1 that all concentration values of the reagents are rather small; more concentrate solutions would lead to a much too rapid process for an accurate detection of the end-point with the employed device.

According to rate laws (2) and (6), the iodide content of the reaction mixture should not affect reaction times ***t***, that is values of k_{cat}/k_{un}. The same conclusion can be drawn from Table 1; the slight differences are probably due to the slight changes in pH and ionic strength of the mixture. Results in Table 1 also show that regardless the iodide content, lower ascorbic acid concentrations induce a better sensitivity. Lower concentrations of the "scavenger" for iodine also correspond to smaller extents of the reaction. Further, as expected from the expressions of k_{un} and k_{cat}, the acid brings about the most significant changes. It is obvious that the best experimental conditions, giving the highest sensitivity for molybdenum, imply the following reagent concentrations: $1.2x10^{-2}$ mole.dm^{-3} H_2O_2, $6x10^{-3}$ mole.dm^{-3} KI, $6x10^{-2}$ mole.dm^{-3} H_2SO_4 and $4x10^{-4}$ mole.dm^{-3} $Na_2C_6H_6O_6$ (see Table 1).

Individual reaction time ***t*** and mean t_0/t values obtained under these circumstances are presented in Table 2. One may observe that replicate runs give repeatable results. A concentration range of Mo(VI) up to 10^{-6} mole.dm^{-3} was covered. The following calibration line t_0/t *vs* catalyst concentration was obtained:

$$t_0/t = (1.01 \pm 0.02) + (6.81 \pm 0.26)x10^5x[Mo(VI)] \quad (R=0.999) \qquad (9)$$

Its correlation coefficient is very good and for all points RSd is less than 2 %. The statistically computed intercept, corresponding to the absence of the catalyst, approaches very well the theoretical value of unity in equation (8). The detection limit was estimated according to IUPAC recommendations [42] and is of $2.5x10^{-8}$ mole.dm^{-3} (2.4 μg.dm^{-3}) Mo(VI).

Vanadium

The same principle was applied to find the optimal experimental conditions for catalysis by V(V). It was found that only ascorbic acid, that is the reaction extent, affects significantly the sensitivity towards vanadium. Reaction conditions,

at 293 ± 0.1 K, to ensure its highest value are: $1x10^{-2}$ mole.dm^{-3} H_2O_2, $5x10^{-3}$ mole.dm^{-3} KI, 0.125 mole.dm^{-3} H_2SO_4 and $8.5x10^{-4}$ mole.dm^{-3} $C_6H_8O_6$. Individual reaction time ***t*** and ***t_0/t*** values recorded under these circumstances are presented in Table 3. Again, replicate runs are repeatable.

Table 3

Results of kinetic runs. Calibration for V(V).
$1x10^{-2}$ mole.dm^{-3} H_2O_2, $5x10^{-3}$ mole.dm^{-3} KI, 0.125 mole.dm^{-3} H_2SO_4,
$8.5x10^{-4}$ mole.dm^{-3} $C_6H_8O_6$ and ionic strength of 0.15 mole.dm^{-3} at 293 ± 0.17 K.

10^5 x [V(V)] (mole.dm^{-3})	0.00	1.25	2.50	5.00	7.50	10.00	12.50
t_0/t	0.998	1.172	1.383	1.732	2.175	2.432	3.049
	1.000	1.175	1.378	1.725	2.186	2.474	3.070
	1.002	1.173	1.381	1.738	2.209	2.400	2.965

The covered concentration range is $1.25x10^{-5} \div 1.25x10^{-4}$ mole.dm^{-3} V(V). The equation of the obtained calibration line is:

$$t_0/t = (0.98 \pm 0.08) + (1.57 \pm 0.12)x10^4x[V(V)] \quad (R=0.996) \quad (10)$$

A good correlation coefficient and agreement between the computed and the theoretical intercepts can be noticed again. The detection limit is of $2.1x10^{-6}$ mole.dm^{-3} (0.1 mg.dm^{-3}) V(V).

Copper and iron

Because one of our goals was the determination of molybdenum and vanadium in the presence of interferents, no attempts were made to find experimental conditions that give best selectivity towards copper and iron. Therefore, optimal conditions for analysis of Mo(VI) and V(V) were taken over. Table 4 presents the values of t_0/t for both Cu(II) and Fe(III). Experiments for Cu(II) were performed in both conditions for Mo(VI) and V(V); while covered concentration ranges covered up to 10^{-5} mole.dm^{-3} and 10^{-4} mole.dm^{-3} Cu(II), respectively. Kinetic runs for Fe(III) were performed only under the optimal circumstances for molybdenum. The covered range was up to 10^{-5} mole.dm^{-3}.

Table 4

Results of kinetic runs. Calibration for Cu(II) and Fe(III).

Calibration for Cu(II). Optimal experimental conditions of Mo(VI) – Table 2						
10^6 x [Cu(II)] (mole.dm^{-3})	0.00	2.00	4.00	6.00	8.00	10.00
t_0/t	1.002 1.000 0.998	1.420 1.419	1.828 1.851	1.909 1.925	2.079 2.064	2.371 2.394
Calibration for Cu(II). Optimal experimental conditions of V(V) – Table 3						
10^5 x [Cu(II)] (mole.dm^{-3})	0.00	1.25	2.50	5.00	7.50	10.00
t_0/t	1.002 1.000 0.998	1.061 1.049 1.027	1.038 1.029 1.034	1.054 1.050 1.048	1.056 1.066 1.060	1.071 1.070 1.073
Calibration for Fe(III). Optimal experimental conditions of Mo(VI) – Table 2						
10^6 x [Fe(III)] (mole.dm^{-3})	0.00	2.00	4.00	6.00	8.00	10.00
t_0/t	1.002 1.000 0.998	1.476 1.481	2.348 2.348	2.750 2.784	3.448 3.500	6.365 6.197

The following calibration lines were obtained for copper:

$$t_0/t = (1.05 \pm 0.08) + (1.35 \pm 0.13)x10^5x[Cu(II)] \quad (R=0.995) \qquad (11)$$

and $$t_0/t = (1.00 \pm 0.01) + (6.90 \pm 2.55)x10^2x[Cu(II)] \quad (R=0.966) \qquad (12)$$

under optimal circumstances for Mo(VI) and V(V), respectively. Because of the steeper slope in equation (11), it is obvious that favorable conditions for the catalysis by Mo(VI) are also more convenient for the catalysis by Cu(II). Even though the studied concentration range is some orders of magnitude smaller than that in the case of V(V), the slope is much higher. Hence the detection limits of the two sets of experimental conditions will also differ considerably: $3x10^{-7}$ mole.dm^{-3} (20 μg.dm^{-3}) and $7.4x10^{-6}$ mole.dm^{-3} (0.5 mg.dm^{-3}) Cu(II) according to equations (11) and (12), respectively.

The calibration line for iron is:

$$t_0/t = (0.93 \pm 0.17) + (3.26 \pm 0.28)x10^5x[Fe(III)] \quad (R=0.996) \qquad (13)$$

Its detection limit is of $5.6x10^{-7}$ mole.dm^{-3} (31 μg.dm^{-3}) Fe(III).

The slopes of calibration lines (11) and (13), corresponding to catalysis by Cu(II) and Fe(III) respectively, are smaller but still comparable to that in equation (9), corresponding to catalysis by Mo(VI) under identical experimental circumstances. This can explain the strong interference by the two ions in the determination of molybdenum.

Bi-component calibration. Vanadium – copper mixtures

In order to study the joint catalytic effect of the vanadium – copper couple, the ions were added together to the reaction mixture. In the presence of constant Cu(II) concentration, the content of V(V) was increased stepwise.

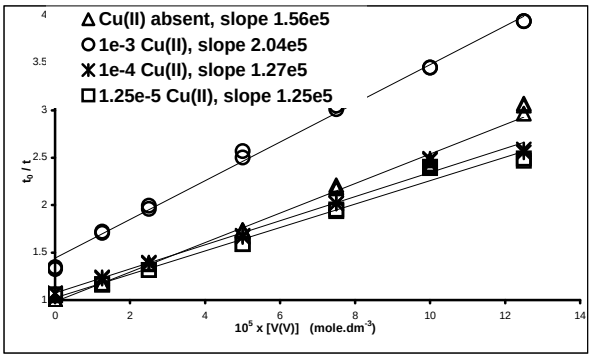

Fig. 1. t_0/t *vs* V(V) concentration for various Cu(II) contents.
Other experimental conditions are the same as listed for Table 3.

Figure 1 presents experimental t_0/t values plotted against [V(V)], for various Cu(II) contents. Although the lines corresponding to 1.25×10^{-5} and 10^{-4} mole.dm^{-3} Cu(II) have practically equal slopes, they lay under the line of "pure" vanadium. On the other hand, a very high content of copper, as compared to that of vanadium, seems to enhance the catalytic effect of the later. This phenomenon may also be due to the fact that Cu(II) promotes the side reaction of H_2O_2 decomposition, so that its contribution to the overall H_2O_2 consumption rate will be more significant. Still, because the extent of process (1) is of 8 %, the linearity of the plot is maintained. To restate, it is obvious that the cumulative catalytic effect of the V(V)-Cu(II) couple is neither additive (lines in Figure 1 are not parallel) nor synergistic.

Therefore, a tri-dimensional t_0/t = f {[V(V)],[Cu(II)]} representation to generate a calibration surface is required for this bi-component matrix. Figure 2 presents the surface of t_0/t values recorded for both stepwise increased vanadium and copper contents. Because t_0/t did not vary significantly for small concentration steps, the surfaces are described by rather few points and are therefore quite "edgy". Figure 2a shows the case of equivalent covered concentration ranges, of up to 10^{-4} mole.dm^{-3}. However, the Cu(II) content was extended to values of two orders of magnitude higher (till 2.5×10^{-3} mole.dm^{-3}) than that of of V(V). This is why, in Figure 2b where all experimental results are presented, a logarithmic concentration scale was chosen for Cu(II). Both Figures 1 and 2b prove that as long as the contents in vanadium and copper are comparable, no dramatic changes of the incubation times occur. But as soon as [Cu(II)] exceeds 5×10^{-4} mole.dm^{-3}, the rate of hydrogen peroxide decomposition increases abruptly. As already mentioned, this is probably due to side reactions.

Figure 2a **Figure 2b**

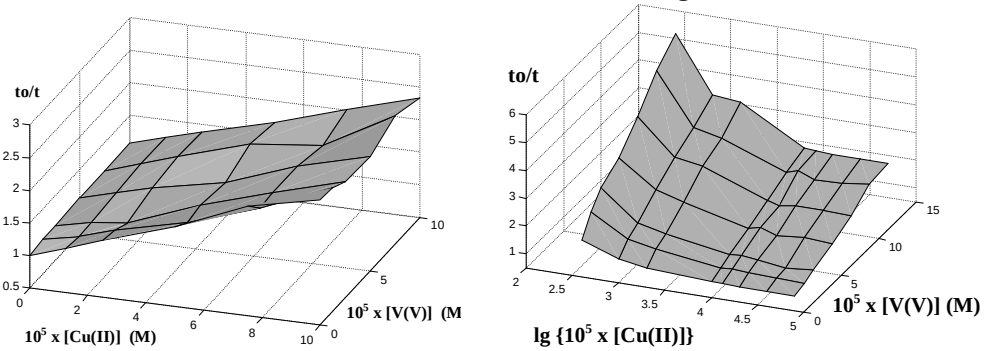

Fig. 2. t_0/t = f {[V(V)],[Cu(II)]} response surfaces for the V(V)-Cu(II) mixture. a) equivalent concentration ranges; b) non- equivalent concentration ranges. Other experimental conditions the same as listed for Table 3.

The supplementary catalytic effect of copper can be suppressed by masking it with EDTA. Table 5 presents average t_0/t values, recorded both in the absence (column A) and presence (columns B and C) of 10^{-5} mole.dm^{-3} Cu(II) and 10^{-3} mole.dm^{-3} EDTA. It is obvious that values in Column C are practically equal to those corresponding to catalysis by only V(V).

To perform a bi-component V(V)-Cu(II) analysis, two distinct kinetic runs are required. The first experiment, carried out in the presence of EDTA, will generate a t_0/t consistent with catalysis by only vanadium. From calibration line (10), its exact concentration can be calculated. The second experiment will lead to a t_0/t value consistent with catalysis by both ions. By cutting the appropriate surface in Figure 2 with a plane, drawn parallel to the XOY plane at the t_0/t value of the unknown sample, a concentration level curve will be obtained. This corresponds to all V(V)-Cu(II) concentration couples that generate the cumulative t_0/t in the second experiment. With the already known V(V) concentration, that of Cu(II) can be easily determined. Figure 3 presents five examples of such level curves at arbitrary taken t_0/t values.

Table 5

Kinetic runs in the presence of EDTA; 10^{-5} mole.dm^{-3} Cu(II) (columns B and C); 10^{-3} mole.dm^{-3} EDTA (column C). Experimental conditions as listed for Table 3.

10^5 x [V(V)] (mole.dm^{-3})	**t_0/t**		
	A	**B**	**C**
0.75	1.100	1.145	1.085
2.50	1.375	1.935	1.378
7.50	2.129	2.460	2.139
12.50	2.860	3.287	2.849

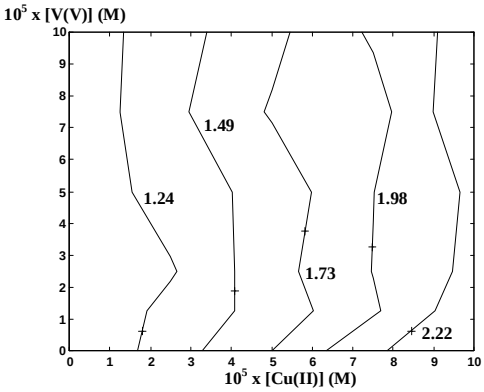

Fig. 3. Examples of concentration level curves corresponding to the surface in Figure 2a.

Tri-component calibration. Molybdenum – copper – iron mixtures

In order to study the joint catalytic effect of the molybdenum – copper – iron mixture, the ions were added together to the reaction mixture. Their concentration was increased stepwise and t_0/t = f {[Cu(II),Fe(III)]} values were recorded, first in the absence of molybdenum and then in the presence of it.

Figure 4 presents the t_0/t values plotted against [Cu(II)] for various Fe(III) contents, in the absence of molybdenum. Because of some parallel lines, it is obvious that the cumulative catalytic effect of Cu(II)-Fe(III) couple is additive only for concentrations under $4x10^{-6}$ mole.dm^{-3} for both ions. Beyond this value their joint effect is neither additive nor synergistic. The same conclusion may be drawn also from Figure 5, that is the response surface t_0/t = f {[Cu(II),Fe(III)]} in the absence of Mo(VI).

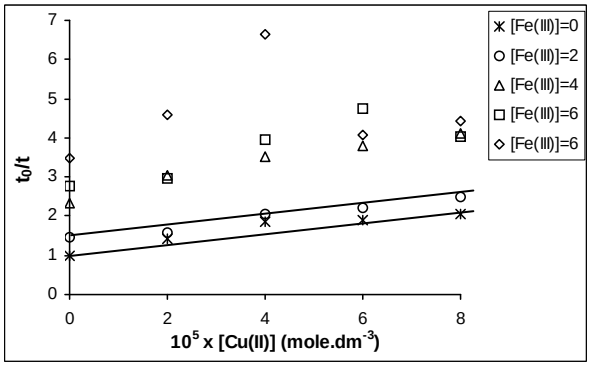

Fig. 4. t_0/t *vs* Cu(II) concentration for various Fe(III) contents given in 10^{-6} mole.dm^{-3}. Molybdenum is absent. Other experimental conditions are the same as listed for

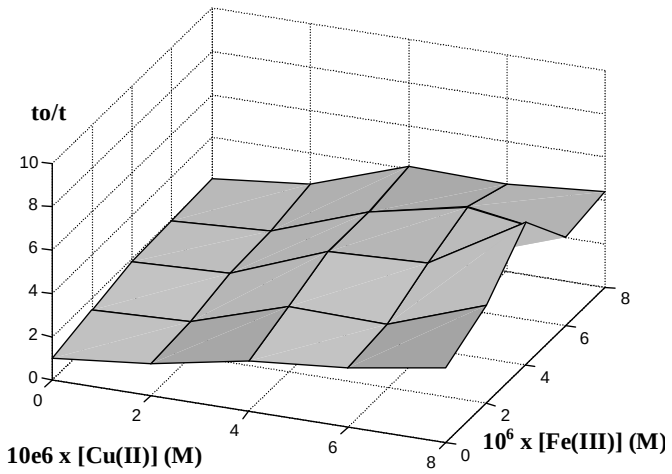

Fig. 5. t_0/t = f {[Cu(II)],[Fe(III)]} response surface in the absence of molybdenum. Other experimental conditions the same as listed for Table 2.

By increasing the Mo(VI) content of the mixture, a family of calibration surfaces was obtained. Their superposition is presented in Figure 6 and stands for the tri-component Mo(VI)-Cu(II)-Fe(III) calibration. Again, because t_0/t did not vary significantly for small concentration steps, each surface is described by only 25 points and has therefore quite sharp edges and angles.

The picture in Figure 6 shows that even though higher t_0/t values are sensed for higher catalyst concentrations, the surfaces lay on top of each other forming a multi-layer body, only for both copper and iron concentrations smaller than 4×10^{-6} mole.dm^{-3}, regardless of the amount of molybdenum present in the mixture. This is probably due to the additive catalytic effect, applying only for narrow concentration ranges, of the Cu(II)-Fe(III) as well as of the Mo(VI)-Cu(II) and Mo(VI)-Fe(III) [38] couples. Moreover, high Cu(II) and Fe(III) contents will favorably influence the side reaction of H_2O_2 decomposition; so that, because it is catalyzed by Fe(III) and promoted by Cu(II), it may significantly affect the overall reaction rate (6). These phenomena may all contribute to the fact that when higher catalyst amounts are present in the sample, the same t_0/t is measured for totally different concentration triplets and the surfaces will cut each other as it may be observed from Figure 6.

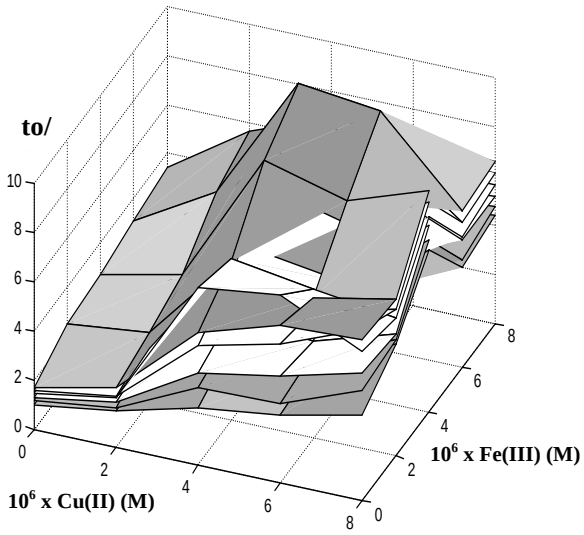

Fig. 6. Tri-component calibration.The family of t_0/t = f {[Cu(II)],[Fe(III)]} response surfaces for $2x10^{-7}$, $4x10^{-7}$ mole.dm^{-3}, $6x10^{-7}$, $8x10^{-7}$ and $10x10^{-7}$ mole.dm^{-3} Mo(VI). Other experimental conditions are the same as listed for Table 2.

The calibration model to be elaborated is based on the t_0/t measurements for known triplets of [Mo(VI)], [Cu(II)] and [Fe(III)]. Its purpose is to function in a reversed way: it will have to give some information about the unknown ion concentrations for a measured t_0/t value of an unknown sample.

The concentration of Mo(VI), like in the case of V(V), can be obtained by means of a distinct experiment. If EDTA is added to the reaction mixture, it will mask the cationic catalysts. Hence, the measured t_0/t value will depend only on the Mo(VI) content of the sample. By using the calibration line of equation (9), its concentration can be determined.

In order to gain some information about the Cu(II) and Fe(III) contents, a t_0/t = f {[Cu(II),Fe(III)]} surface for the exact found [Mo(VI)] is needed. Again, the intersection of this surface with a plane, drawn parallel to the XOY plane at the t_0/t value of the unknown sample, will generate some level curves. These correspond to the Cu(II)–Fe(III) concentration couples to generate the experimentally determined t_0/t, for a certain Mo(VI) content. Figure 7 presents 15 examples of such curves obtained in the absence of Mo(VI), by cutting the surface in Figure 5 with the same number of arbitrary chosen planes. As it may be observed, the exact concentrations of Cu(II) and Fe(III) may not be established, the curves will indicate only a range of values (a minimum and a maximum).

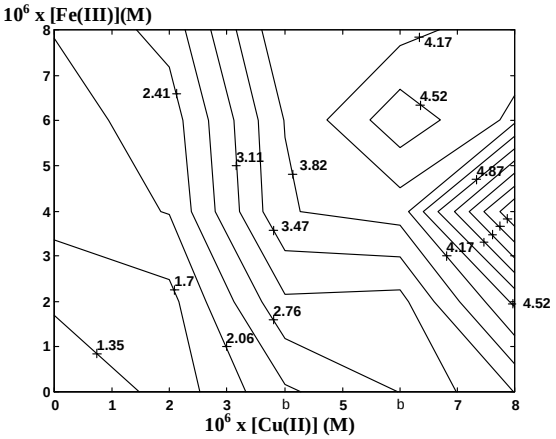

Fig. 7. Examples of concentration level curves corresponding to the surface in Figure 5.

In order to construct an appropriate t_0/t = f {[Cu(II),Fe(III)]} calibration surface at any Mo(VI) concentration within the range of concentrations of up to 10^{-6} mole.dm^{-3}, we employed an artificial neural network (ANN) [43,44]. The surface has to be much smoother than those in Figures 5 and 6, thus described by much more points.

To resume, the proposed calibration model would consist of both the calibration line (9), and a t_0/t = f {[Cu(II),Fe(III)]} surface generated by an ANN. In order to elaborate such a model, an artificial neural network was trained by using 115 sets of experimental data t_0/t = f {Mo(VI)],[Cu(II)],[Fe(III)]}. Its characteristics are listed in Table 6. A Levenberg–Marquardt learning algorithm [45] was employed for 60 epochs till the sum squared error reached a satisfactory predetermined value. Testing was performed with 10 sets of data.

To evaluate the prediction capacity of the network, calculated data Y were plotted against experimental data X, for both the training and the testing set of values. The equations of the obtained lines are:

$$Y = 0.117 + 0.974\ X \qquad (R = 0.987) \qquad (14)$$

and

$$Y = 0.079 + 0.980\ X \qquad (R = 0.985) \qquad (15)$$

respectively. Both have rather good correlation coefficients, intercepts close to zero and slopes close to unity (ideal values). Thus, the simulation capacity of the ANN is expected to be rather good.

The trained network was further used to generate, by means of simulation, the replicate of the t_0/t = f {[Cu(II),Fe(III)]} surface in Figure 5. The obtained result is presented in Figure 8.

Table 6

Characteristics of the artificial neural network

Parameter	Value
Input nodes	3
Output nodes	1
Hidden layers	1
Hidden nodes	7
Input layer transfer function	Identity
Hidden layer transfer function	Sigmoid: $f(x) = 1/\left(1+e^{-x}\right)$
Output layer transfer function	Sigmoid: $f(x) = 1/\left(1+e^{-x}\right)$
Bias	Variable
Learning rate	Variable

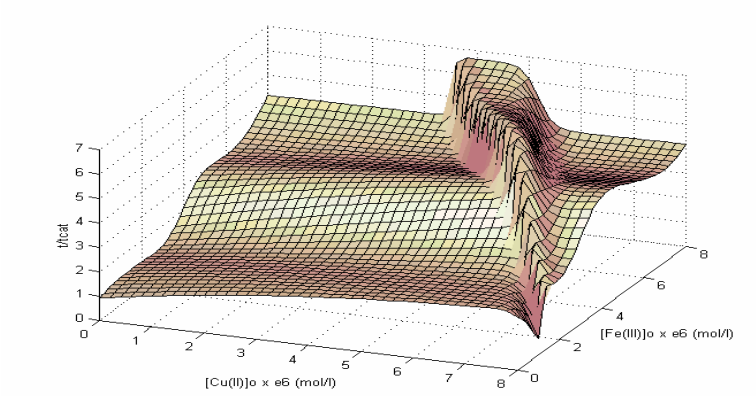

Fig. 8. ANN generated t_0/t = f {[Cu(II),Fe(III)]} calibration surface in the absence of molybdenum. The chosen concentration step is of $2x10^{-7}$ mole.dm^{-3}.

It is obvious that the two surfaces, the experimental one in Figure 5 and the simulated one in Figure 8, do not match. The latter exhibits a steep increase exactly in the region of concentrations where the response surfaces in Figure 6 cut each other. Only for Cu(II) and Fe(III) concentrations smaller than $4x10^{-6}$ mole.dm^{-3}, do simulated data approximate measured ones.

As a result, because in a certain range of catalyst concentrations their cumulative effect is completely nonlinear and completely different sets of inputs correspond to the same output, none of the surfaces obtained by means of simulation by this ANN are suitable in the proposed calibration model. However, in a more narrow concentration range of copper and iron, where experimental response surfaces lay one on the top of each other, an artificial neural network could be employed in calibration. In this case an other ANN, with different

characteristics, has to be trained, tested and used for generating the required t_0/t = f {[Cu(II),Fe(III)]} surfaces. Unfortunately, there is not enough available experimental data, for [Cu(II)] and [Fe(III)] less than $4x10^{-6}$ mole.dm^{-3}, to do so.

Potentiometric detection of the end-point

Because visual detection of the reaction's end-point is a monotonous and tedious process, the accuracy of the results may be questioned. Therefore, potentiometric verification of the calibration line (19) for molybdenum was performed. Moreover, some results for Mo(VI)-Cu(II) and Mo(VI)-Fe(III) couples were also compared. It is worth mentioning that the water to prepare these solutions was more pure (contained no ionic residuals) than that used for previous experiments, so that results may be affected. In order to have a basis for comparison potentiometric measurements were doubled by visual detection, under identical reaction conditions and by using the same reagent solutions.

During these experiments, the electromotive force of the

$$Hg / Hg_2Cl_2 / Cl^- (sat) // I^- / EMIS - I$$

electrochemical cell was monitored versus time. Typical kinetic runs are presented in Figure 9 for both the absence (the blank) and the presence of 10^{-6} mole.dm^{-3} Mo(VI). The plots have the shape of titration curves. For the simplicity of computing, the end-point of the reaction was considered to correspond to the inflection point of the curve. The time at which it occurred, was considered to be the searched for incubation time.

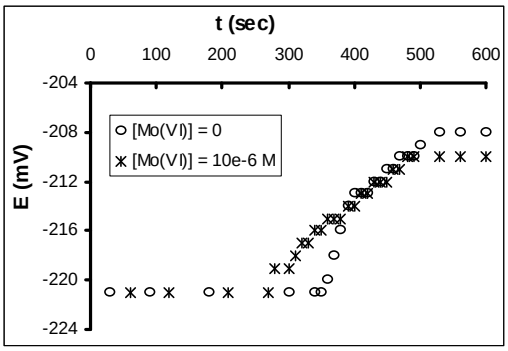

Fig. 9. Typical potentiometric kinetic runs. Experimental conditions as listed for Table 2.

Values of the individual t_0/t ratios for potentiometric detection of the reaction time t were plotted against the values obtained by visual detection. Some selected results are presented in Figure 10. It is obvious that the kinetic runs are repeatable and the two methods give comparable results.

The equations of the obtained calibration lines are:

$$t_0/t = (0.97 \pm 0.05) + (4.04 \pm 0.83)x10^5x[Mo(VI)] \quad (R=0.990) \qquad (16)$$

and

$$t_0/t = (0.99 \pm 0.03) + (3.77 \pm 0.46)x10^5x[Mo(VI)] \quad (R=0.992) \qquad (17)$$

for potentiometric and visual detection of incubation time, respectively. The lines have good and comparable correlation coefficients. Their intercepts and slopes are also in good agreement. However, both slopes are somewhat smaller than 6.81×10^5 in equation (9). This is due to the fact that the water used to prepare the reagent solutions was more pure in these cases. It was demineralized as well as four times distilled, while the water used in previous experiments was only twice distilled. We suspect that is also contained some residual amounts of ions with catalytic activity towards the indicator reaction. This fact was confirmed by other kinetic experiments in our laboratory, too.

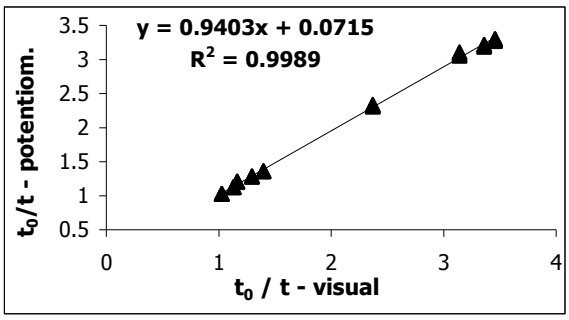

Fig. 10. Potentiometric *versus* visual detection of the end-point.

By taking into account the experimental data in Figure 10 as well as the calibration equations (16) and (17), it may be concluded that the two methods have comparable performances.

Acknowledgments. The authors thankfully acknowledge Dr. Ing. Nagy Zoltan for developing the necessary ANN software as well as for the financial support of the CNCSIS – Romanian Ministry of Education, Grant No 46174/27.11.1997, codes no 10 and Grant No 32575/1999, code no 40/113.

REFERENCES

1. J.-M. M e r m e t, M. O t t o, H.M. Widmer (eds.), *Analytical Chemistry*, Wiley-VCH, Weinheim, Chap. 6, **1998**, pg. 227-252.
2. A. A. N o y e s, W. O. S c o t t, *Z. Phys. Chem*., **1895**, *18*, 118; G. B r e d l g, J. H. W a l t o n, *Z. Elektrochem.,* **1903***, 9*, 114; J. H. W a l t o n, *Z. Phys. Chem*., **1904**, *47*, 184; K., O k a b e, *J. Chem. Soc. Japan*, **1940**, *61*, 1235; M. A. G a r b a l l o, *Anales Assoc. Qcim., Arg.*, **1948**, *36*, 150; M. K a t a o k a, Y. Y o s h i z a w a, T. K a m b a r a, *Bunseki Kagaku*, **1982**, *31*, E171.
3. H. L lie b ha f s k y, A. M o h a m m e d, *J. Amer. Chem. Soc*., **1933**, *55*, 3977.

4. G. S v e h l a, L. E r d e y, *Mikorochem J.,* **1963**, *7*, 206.
5. G. S v e h l a, *Analyst*, **1969**, *94*, 1120.
6. K. B. Y a t s i m i r s k i i, *A kemai analízis kinetikus módszerei*, Akadémiai Kiadó, Budapest, **1966**, pg. 71-83.
7. K. B. Y a t s i m i r s k i i, MTP, *International Review of Science, Physical Chemistry* Series One, Vol. 12, *Analytical Chemistry*, part 1, University Park Press, Baltimore, London, **1973**, pg. 193-217.
8. H. A. M o t t o l a, *Kinetic Aspects of Analytical Chemistry* (Vol. 96 of the series "*Chemical Analysis*"), John Wiley & Sons, New York, **1988**, Chapter 2, pg. 24-52.
9. H. M ü l l e r, *CRC Crit. Rev. Anal. Chem*., **1982**, *13*, 313.
10. G. S v e h l a, L. E r d e y, *Mikrochem. J*., **1963**, *7*, 221.
11. H. W e i s z, H. L u d w i g, *Anal. Chim. Acta*, **1975**, *75*, 181.
12. H. M ü l l e r, P. N e n n i n g, S. A r t m a n n, *2nd Symp. Anal Solid State Mater*., Karl-Marx Stadt, Germany, **1978**; H. M ü l l e r, *CRC Crit. Rev. Anal. Chem*., **1982**, *13*, 313.
13. B. F. Q u i n n, P. H. W o o d s, *Analyst*, **1979**, *104*, 552.
14. M. K a t a o k a, K. N i s h i m u r a, T. K a m b a r a, *Talanta*, **1983**, *30*, 941.
15. Z. F a n g, S. X u, *Anal. Chim. Acta*, **1983**, *145*, 143.
16. J. A. A m b e r s o n, G. S v e h l a, *Anal. Chim. Acta*, **1985**, *178*, 255.
17. H. Dacka-Seliga, *Chem. Anal. (Warsaw)*, **1985**, 30, 881.
18. J. T. K e n n e d y, G. S v e h l a, *Fresenius' Z. Anal. Chem*., **1986**, *324*, 19.
19. M. T r o j a n o w i c z, A. H u l a n i c k i, W. M a t u s z e w s k i, M. P a l y s, A. F u k s i w i c z, T. H u l a n i c k a – M i c h a l a k, S. R a s z e w s k i, J. S z y l l e r, W. A u g u s t y n i a k, *Anal. Chim. Acta*, **1986**, *188*, 165.
20. Z. Y u, Y. L i, *Fenxi Huaxue*, **1987**, *15*, 841; H. A. M o t t o l a, D. P é r e z – B e n d i t o, H. B. M a r k, Jr., *Anal. Chem*., **1990**, *62*, 441R.
21. L. C. R. P e s s e n d a, A. O. J a c i n t h o, E. A. G. Z a g a t t o , *Anal. Chim. Acta*, **1988**, *214*, 239.
22. R. M. V i l l a n u e v a, I. D. M a r t i n e z, G. R a m i s, M. C. G a r c i a, *Thermochim. Acta*, **1990**, *158*, 215.
23. C. Z h u a n g, S. F u, *Fenxi Ceshi Tongbao*, **1990**, *9*, 39; H. A. M o t t o l a, D. P é r e z – B e n d i t o, *Anal. Chem*., **1992**, *64*, 407R.
24. D. L i u, A. Z h a n g, *Yingyang Xuebao*, **1991**, *13*, 68; *Chem. Abstr.*, **1991**, *115*, 269443u.
25. J. C. A n d r a d e, S. P. E i r a s, R. E. B u r n s, *Analyst*, **1993**, *118*, 213; J. C. A n d r a d e, S. P. E i r a s, R. E. B u r n s, *Anal. Chim. Acta*, **1991**, *255*, 149.
26. T. Y a m a n e, Y. A r u g a, T. O g a w a, *Monatsh. Chem*., **1994**, *125*, 20; *Chem. Abstr*., **1994**, *121*, 220560q.
27. E. N. V. M. C a r r i l h o, F. J. K r u g, E. A.G. Z a g a t t o, *Talanta*, **1995**, *42*, 2021.
28. R. N. V o e v u t s k a y a, V. K. P a v l o v a, A. T. P i l i p e n k o, *Zh. Analit. Khim*., **1979**, *34*, 1299.
29. M. K a t a o k a, K. N i s h i m u r a, T. K a m b a r a, *Bunseki Kagaku*, **1983**, *32*, 516; *Analytical Abstracts*, Royal Society of Chemistry, Silver Platter International N.V., Cambridge, UK, 1980-1998/09, Accession Number 4605B00205.

30. M. K a t a o k a, Y. Y o s h i z a w a, T. K a m b a r a, *Bunseki Kagaku*, **1982**, *31*, E171; D. Pérez-Bendito, M. Silva, *Kinetic Methods in Analytical Chemistry*, Ellis Hoorwood Limited, Chichester, **1988**, pg. 49.
31. I. I. A l e k s e e v a, V. V. B o r i s o v a, A. V. S h u g i n i n a, L. T. Y u r a n o v a, *Zh. Analit. Khim*., **1981**, *36*, 108.
32. Q. C a i, R. Y a n g, *Fenxi Huaxue*, **1988**, *16*, 1021, *Analytical Abstracts*, Royal Society of Chemistry, Silver Platter International N.V., Cambridge, UK, 1980-1998/09, Accession Number 5107B00107.
33. A. A l t i n a t a, B. P e k i n, *Anal. Lett.,* **1973**, *6*, 667.
34. R H., H e, J H. W a n g, *Mikrochim. Acta*, **1996**, *124*, 195.
35. R. L i u, D. L i u, A. S u n, G. L i u, *Analyst*, **1995**, *120*, 565.
36. J. W a n g, R. H e, Talanta, **1996**, *43*, 391.
37. C. W i e s e, G. S c h w e d t, *Fresenius' J. Anal. Chem*., **1997**, *358*, 718.
38. I. B â l d e a, C. C ă l i n, *Rev. Chim*., **1998**, *49*, 665.
39. A. R u s t o i u – C s a v d a r i, I. B â l d e a, C. C ă l i n, *Proceedings of the 6th Internat. Symp. On Kinetics in Anal. Chem., KAC'98*, Kassandra, Greece, **1998**, p. 39; A. R u s t o i u – C s a v d a r i, I. B â l d e a, L. C o p o l o v i c i, D. M i h a i, *a XI-a Conferinta Internationala de Chimie si Inginerie Chimica,* Bucureşti, România, **1999**.
40. C. H. B a m f o r d, C. F. H. T i p p e r (eds.), *Comprehensive Chemical Kinetics*, Elsevier, Amsterdam, Vol.6, **1972**, pg. 406.
41. G. N i a c, V. V o i c u l e s c u, I. B â l d e a, M. P r e d a, *Formule, tabele, probleme de chimie fizică*, Ed. Dacia, Cluj-Napoca, **1984**, pg. 264.
42. Analytical Method Committee, *Analyst*, **1987**, *112*, 199.
43. F. D e s p a g n e, D. L. M a s s a r t, *Analyst*, **1998**, *123*, 323.
44. A. R u s t o i u – C s a v d a r i, L. C o p o l o v i c i, Z. N a g y, *Proceedings of the 14th International Congress of Chemical and Process Engineering* (on CD-ROM), Praha, Czech Republic, **2000**, 1447.
45. M. T. H a g a n, M. M e n h a j, *IEEE Transactions on neural Networks*, **1994**, *5*, 989.